DALTON

A water-stable and strongly luminescent self-assembled non-covalent lanthanide podate †

Carine Edder,[a] Claude Piguet,*[,a] Jean-Claude G. Bünzli*[,b] and Gérard Hopfgartner[c]

[a] *Department of Inorganic, Analytical and Applied Chemistry, University of Geneva, 30 quai E. Ansermet, CH-1211 Geneva 4, Switzerland*
[b] *Institute of Inorganic and Analytical Chemistry, University of Lausanne, BCH 1402, CH-1015 Lausanne-Dorigny, Switzerland*
[c] *F. Hoffmann-La Roche Ltd, Pharmaceuticals Division, Department of Drug Metabolism and Kinetics, CH-4070 Basle, Switzerland*

The segmental ligand 2-(6-carboxypyridin-2-yl)-1,1′-dimethyl-2′-(5-methylpyridin-2-yl)-5,5′-methylenebis(1*H*-benzimidazole) (L^9) reacted with an equimolar mixture of Ln^{III} (Ln = La or Eu) and Zn^{II} in basic conditions to give selectively the self-assembled dinuclear non-covalent podates $[LnZn(L^9 - H)_3]^{2+}$. Electrospray mass spectrometry and proton NMR spectroscopy show that $[LnZn(L^9 - H)_3]^{2+}$ adopt the expected head-to-head triple-helical structure with Zn^{II} pseudo-octahedrally co-ordinated by the bidentate binding units of the three segmental ligands and Ln^{III} occupying the remaining facial pseudo-tricapped trigonal prismatic site produced by the wrapped unsymmetrical tridentate units. Upon UV irradiation, solutions of $[EuZn(L^9 - H)_3]^{2+}$ in acetonitrile or in water produce strong red luminescence. The Eu ($^5D_0$) lifetime and quantum yield indicate that Eu^{III} is efficiently protected from external interactions for complex concentration in the range 10^{-4}–10^{-8} M and that no solvent molecule enters the first co-ordination sphere. Electrospray mass spectrometry combined with high-resolution emission spectroscopy confirm that the structure of the dinuclear triple-helical complex $[EuZn(L^9 - H)_3]^{2+}$ is maintained at low concentration which strongly contrasts with the lipophilic analogous non-covalent lanthanide podates $[EuZn(L^i)_3]^{5+}$ {$i = 7$ or 8; 2-[6-(organo)pyridin-2-yl]-1,1′-dimethyl-2′-(5-methylpyridin-2-yl)-5,5′-methylenebis(1*H*-benzimidazole)} which are decomplexed in acetonitrile for concentrations below 10^{-5} M. Detailed photophysical studies have established that $[EuZn(L^9 - H)_3]^{2+}$ works as an efficient UV ⟶ VIS light-converting device in the solid state and in water.

Semi-rigid aromatic tridentate ligands are well suited for the co-ordination of lanthanide(III) metal ions, Ln^{III}, because they display large chelate effects and lead to nine-co-ordinate tricapped trigonal prismatic complexes $[LnL_3]^{3+}$ which match the stereochemical preferences of the cations.[1] Tailored luminescent probes based on symmetrical tridentate units containing a central pyridine ring have attracted much attention,[2–5] and it has been shown that pyridine-2,6-dicarboxylate $[L^1 - 2H]^{2-}$ forms stable and strongly luminescent three-bladed propellers $[Ln(L^1 - 2H)_3]^{3-}$ upon reaction with Ln^{III} metal ions.[5] However, a limited structural and electronic control of the co-ordination sphere around Ln^{III} is possible with L^1 because no substituents can be connected to the carboxylic side arms. In an effort to improve the structural control, rigid 2,2′:6′,2″-terpyridine units L^5 and L^6 have been treated with Ln^{III} to give 1:3 mononuclear triple-helical complexes $[Ln(L^i)_3]^{3+}$ ($i = 5$ or 6).[6,7] As only nine weak Ln–N (heterocyclic) dative bonds exist in $[Ln(L^5)_3]^{3+}$, fast on–off equilibria of the distal pyridine rings are observed in acetonitrile.[6] On the other hand, the improved preorganization in L^6 produces stable and inert $[Ln(L^6)_3]^{3+}$ complexes in acetonitrile.[7] Recent detailed investigations of analogous symmetrical tridentate receptors possessing carboxamide (L^2),[8] ester (L^3)[9] or benzimidazole (L^4)[10] side arms have led to the conclusion that the simultaneous control of thermodynamic, structural and electronic properties in the triple-helical lanthanide building blocks $[Ln(L^i)_3]^{3+}$ requires the design of unsymmetrical tridentate binding units.[1] As a first step toward this goal, an unsymmetrical 2,6-bis(benzimidazole)-pyridine unit related to L^4 has been connected to a bidentate unit coded for the recognition of pseudo-octahedral d-block ions in L^7. Using the highly selective self-assembly processes developed for helicates,[11] we were able to prepare the head-to-head triple-stranded heterotopic helicates (HHH)-$[LnZn(L^7)_3]^{5+}$ for ligand concentrations larger than 10^{-2} M.[12] In the latter complexes, termed non-covalent lanthanide podates, Zn^{II} occupies the pseudo-octahedral site produced by the three wrapped strands which corresponds to a non-covalent tripod organizing the unsymmetrical tridentate binding units for their facial co-ordination to Ln^{III}. Improved selectivity, stability and luminescence quantum yield result from the replacement of the terminal benzimidazole ring in L^7 by a carboxamide group in L^8.[13] Considering the beneficial effect of carboxylate groups to provide stable, water-resistant and luminescent Ln^{III} complexes with acyclic[2–5] and macrocyclic[14] receptors, we have planned to introduce this functional group into the segmental ligand L^9. In this paper, we report on the synthesis of L^9 and on the first self-assembled non-covalent lanthanide podate (HHH)-$[EuZn(L^9 - H)_3]^{2+}$ which is stable and strongly luminescent in water, a crucial point if these probes are to be used in biological media.[15]

Results and Discussion

Syntheses of L^9 and its complexes

Compound L^8 is obtained in eleven steps according to a recently developed synthetic strategy.[13] The selective hydrolysis of the tertiary amide group according to standard conditions only fails,[16] but harsh basic conditions, previously used for the hydrolysis of polycarboxamide,[17] give L^9 in good yield (91%). Compound L^9 or its deprotonated forms Na[L^9 − H] and

† *Supplementary data available* (No. SUP 57311, 2 pp.): electrospray mass spectra of $[LnZn(L^9 - H)_3]^{2+}$ (Ln = La or Eu). See Instructions for Authors, *J. Chem. Soc.*, *Dalton Trans.*, 1997, Issue 1.

Table 1 Proton NMR shifts (with respect to $SiMe_4$) of L^9, $Na[L^9 - H]$ in $(CD_3)_2SO$ and $[LnZn(L^9 - H)_3]^{2+}$ (Ln = La or Eu) in CD_3CN at 298 K

Compound	Me^1	Me^2	Me^3	H^1	H^2	H^3	H^4	H^5	H^6	$H^{7,8}$	H^9	H^{10}	H^{11}	H^{12}	H^{13}	H^{14}
L^9	2.39	4.32	4.18	8.56	7.79	8.18	7.51	7.23	7.57	4.22	7.62	7.27	7.53	8.12	8.16	8.48
$Na[L^9 - H]$	2.38	4.27	4.16	8.56	7.80	8.14	7.50	7.22	7.56	4.20	7.57	7.22	7.50	7.91	8.14	7.91
$[LaZn(L^9 - H)_3]^{2+}$	2.14	4.09	4.26	7.79	7.80	8.09	7.39	7.12	5.35	3.43, 3.58	6.12	6.92	7.29	8.33	8.04	7.80
$[LaZn(L^8)_3]^{5+}$*	2.15	4.21	4.33	7.74	7.84	8.17	7.61	7.22	5.42	3.53, 3.64	5.82	6.96	7.35	8.52	8.35	7.82
$[EuZn(L^9 - H)_3]^{2+}$	2.59	4.83	2.37	8.66	8.33	8.87	8.16	7.68	9.13	3.96, 4.50	15.95	7.46	6.10	2.56	4.59	3.92
$[EuZn(L^8)_3]^{5+}$*	2.37	4.55	3.75	8.14	8.09	8.52	7.99	7.56	7.31	3.99, 4.16	9.89	7.42	6.06	4.60	6.34	5.46

* Taken from ref. 13.

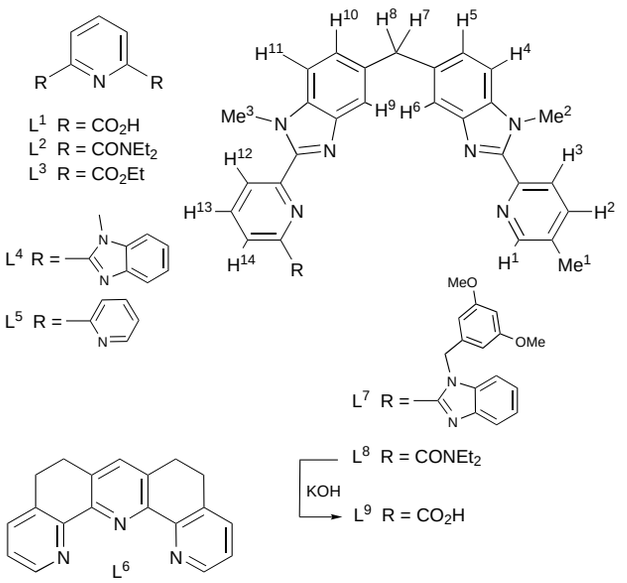

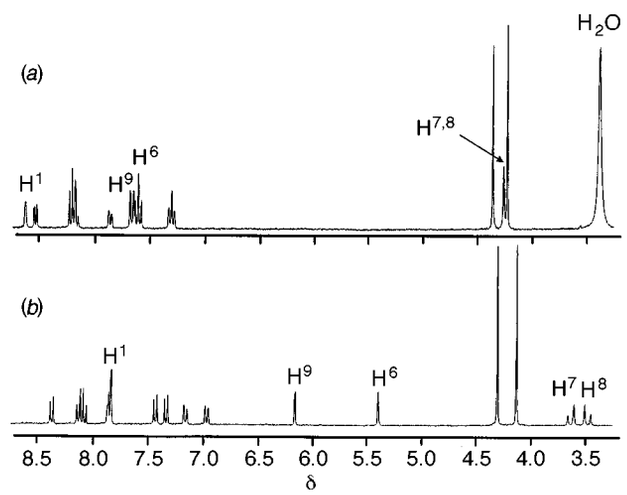

Fig. 1 Proton NMR spectra of (*a*) L^9 in $(CD_3)_2SO$ and (*b*) $[LaZn(L^9 - H)_3]^{2+}$ in CD_3CN

$NBu_4[L^9 - H]$ are insoluble in most common organic solvents and in water. A low solubility (*ca.* 2×10^{-4} M) is observed in dimethyl sulfoxide and nitromethane which strongly limits the preparation of lanthanide complexes. However, a suspension of L^9 (3 equivalents) in nitromethane containing $Ln(ClO_4)_3 \cdot 7H_2O$ (Ln = La or Eu; 1 equivalent), $Zn(ClO_4)_2 \cdot 6H_2O$ (1 equivalent) and triethylamine (3 equivalents) slowly dissolves to give a clear mixture from which the complexes $[LnZn(L^9 - H)_3][ClO_4]_2 \cdot nH_2O$ (Ln = La, $n = 6.6$; Ln = Eu, $n = 7$) can be fractionally crystallized by slow diffusion of diethyl ether. Only moderate yields of pure compounds are obtained (38–43%) because triethylammonium perchlorate co-crystallizes in an excess of diethyl ether. Attempts to synthesize the analogous Gd^{III} complex failed as a result of the lower solubility of the final complex with heavier Ln^{III}. The IR spectra of the complexes show the bands characteristic of the co-ordinated ligands ($\nu_{C=C}$, $\nu_{C=N}$),[13] together with the asymmetrical ν_{CO_2} vibration of the deprotonated carboxylate group at 1630 cm^{-1} and vibrations typical of ionic perchlorates (625, 1090 cm^{-1}).[18]

Solution structure of $[LnZn(L^9 - H)_3]^{2+}$

The poor solubility of the free ligand $[L^9 - H]^-$ and of the non-covalent podates $[LnZn(L^9 - H)_3]^{2+}$ precludes a complete thermodynamic study of the self-assembly process[11,13] and we have thus investigated the structure of the complexes in solution after their isolation in the solid state. The electrospray (ES) mass spectra of 10^{-4} M solutions of $[LnZn(L^9 - H)_3][ClO_4]_2$ in acetonitrile display only peaks corresponding to the cations $[LnZn(L^9 - H)_3]^{2+}$ (*m/z* 833.4, Ln = La; 840.0, Ln = Eu, SUP 57 311) together with the signal of the perchlorate anion (*m/z* = 99.0) in the negative mode. As a result of the low positive charge borne by the cation (2+), we do not observe adducts with the counter anions.[19] Upon dilution to 10^{-5} and 10^{-6} M, the absolute intensity of the signals of $[LnZn(L^9 - H)_3]^{2+}$ shows the expected decrease, but no trace of free deprotonated (or protonated) ligand and homonuclear Zn^{II} complexes are detected. This contrasts with the analogous podates $[LnZn(L^8)_3]^{5+}$ where partial decomplexation is observed at 10^{-5} M leading to the release of significant quantities of free ligand (detected as $[L^8 + H]^+$) and equal amounts of $[Zn(L^8)_2]^{2+}$ and $[Zn(L^8)_3]^{2+}$ in solution under similar conditions according to ES mass spectra.[13] Although L^9 and $[Zn(L^9 - H)_2]$ are neutral and cannot be detected by mass spectrometry, the intense ES mass spectral response expected in presence of traces of $[L^9 - H]^-$ or $[L^9 + H]^+$[19,20] together with the lack of peaks corresponding to $[Zn(L^9 - H)_3]^-$ in the negative mode points to a significantly larger stability for $[LnZn(L^9 - H)_3]^{2+}$ in solution compared to $[LnZn(L^i)_3]^{5+}$ ($i = 7$ or 8).[12,13]

The ^1H NMR spectrum of the diamagnetic non-covalent podate $[LaZn(L^9 - H)_3]^{2+}$ in CD_3CN (5×10^{-4} M) displays 17 signals which implies three equivalent ligands related by a C_3 axis (Table 1, Fig. 1). The NMR signals have been attributed using nuclear Overhauser effects (NOE) and two-dimensional correlation (COSY) spectra. Atoms $H^{7,8}$ are diastereotopic and give an AB spin system compatible with a C_3 point group (excluding symmetry planes)[13] for the complex and a head-to-head arrangement of the three helically wrapped ligands as similarly described for $[LaZn(L^i)_3]^{5+}$ ($i = 7$ or 8).[12,13] The helical twist of the strand is exemplified by the significant upfield shift (with respect to the free ligand L^9) of H^6 (2.22) and H^9 (1.50 ppm) resulting from the particular conformation of the diphenylmethylene spacer which places these protons in the shielding region of the adjacent benzimidazole ring of the same strand.[21] The intrastrand NOE effects [$Me^2 - H^3$, $Me^3 - H^{12}$; Fig. 2(*a*)] clearly establish cisoid conformations of the two pyridine–benzimidazole units within each strand, in agreement with their complexation to Zn^{II} and La^{III}. The observation of a weak, but significant interstrand NOE effect between Me^3 and H^5 is diagnostic for a close interstrand packing interaction associated with a triple-helical arrangement of the ligands [Fig. 2(*b*)].[13] We conclude that $[LnZn(L^9 - H)_3]^{2+}$ adopts a triple-helical struc-

Table 2 Ligand-centred absorption and emission properties in $[LnZn(L^9 - H)_3]^{2+}$ complexes in the solid state and in solution[a]

Compound	$\pi \longrightarrow \pi^*/cm^{-1}$			$^1\pi\pi^*/cm^{-1}$		$^3\pi\pi^*/cm^{-1}$		$\tau(^3\pi\pi^*)/ms$	
L^8[b]		30 770		24 940	20 040	18 870	17 860 (sh)	560 ± 18	41 ± 2
L^9		31 250		24 750	21 980 (sh)	20 620	19 420	1050 ± 30	14 ± 2
$[LaZn(L^8)_3]^{5+}$[b]	32 800 (sh)	31 000		22 600	19 960	19 050	18 000 (sh)	250 ± 4	36 ± 6
$[LaZn(L^9 - H)_3]^{2+}$	41 000 (sh)	30 760		24 210	21 280	19 880	18 690 (sh)	918 ± 5	116 ± 10
$[EuZn(L^8)_3]^{5+}$[b]	32 750 (sh)	30 900	26 000 (sh)	21 480	*c*	*c*	*c*	*c*	*c*
$[EuZn(L^9 - H)_3]^{2+}$	41 000 (sh)	30 760		22 940	*c*	*c*	*c*	*c*	*c*
$[EuZn(L^9 - H)_3)]^{2+}$[d]	41 320 (sh)	30 580	29 250 (sh)	*e*	*e*	*e*	*e*	*e*	*e*
	(61 000)	(91 500)	(67 500)						
$[EuZn(L^9 - H)_3]^{2+}$[f]	40 980 (sh)	30 580	29 200 (sh)	*e*	*e*	*e*	*e*	*e*	*e*
	(62 000)	(92 000)	(68 000)						

[a] Reflectance spectra recorded at 295 K, luminescence data at 77 K and lifetime measurements at 10 K (solution in EtOH, λ_{exc} = 308 nm) in the solid state; sh = shoulder. [b] Taken from ref. 13. [c] $^3\pi\pi^*$ Luminescence quenched by transfer to Ln ion. [d] 10^{-4} M in acetonitrile, ε are given in parentheses in $M^{-1}\ cm^{-1}$. [e] Ligand-centred emissions were not detected in solution. [f] 10^{-4} M in water.

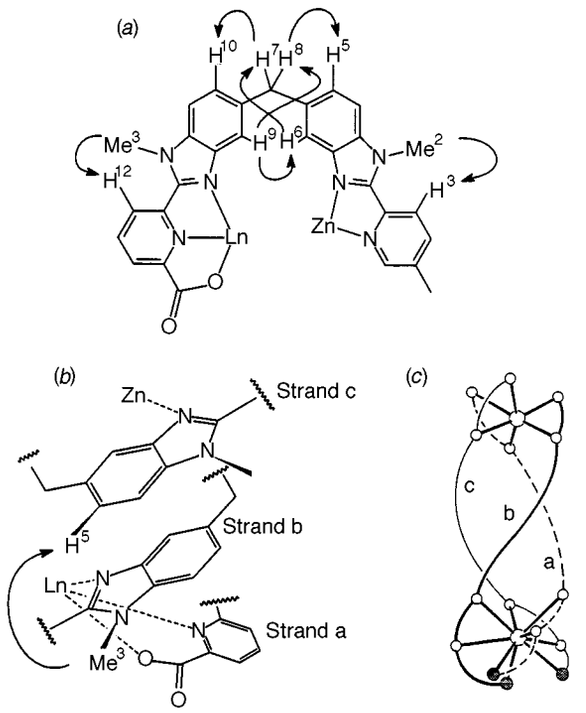

Fig. 2 Selected (*a*) intrastrand and (*b*) interstrand NOE effects and (*c*) triple-helical structure determined by NMR for (HHH)-$[LnZn(L^9 - H)_3]^{2+}$ in CD_3CN

ture similar to that found for $[LnZn(L^8)_3]^{5+}$,[13] except for small differences in the chemical shifts of H^9, H^{12} and H^{13} which are tentatively assigned to minor structural and electronic variations associated with the replacement of the carboxamide in L^8 by a carboxylate group in $[L^9 - H]^-$ [Fig. 2(*c*)]. Possible structural distortions have been addressed using Eu^{III} as an internal NMR magnetic probe in the paramagnetic complex $[EuZn(L^9 - H)_3]^{2+}$. The paramagnetic shift induced at a given nucleus *i* is given by the sum of the contact term (δ_{ij}^c), which results from through-bond Fermi interactions, and a pseudo-contact term (δ_j^{pc}) arising from the residual isotropic dipolar contribution associated with the anisotropic part of the molecular magnetic susceptibility tensor given by equation (1)

$$\delta_{ij}^{pc} = C_j \cdot \frac{a}{T^2} \cdot \frac{1 - 3\cos^2\theta_i}{r_i^3} \qquad (1)$$

for axial lanthanide complexes.[22] The r_i and θ_i are the axial coordinates of the nucleus *i* with respect to the ligand field axes for a ligand field constant *a* at a given temperature *T*, and C_j is the Bleaney coefficient for Ln_j.[23] We have previously established that H^9 in $[EuZn(L^8)_3]^{5+}$ is significantly affected by both contributions, but the induced paramagnetic shift undergone by H^6

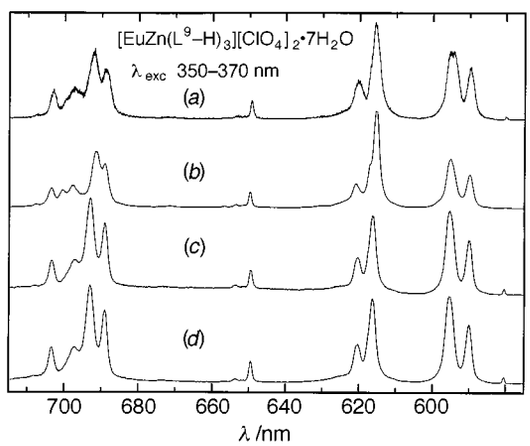

Fig. 3 Emission spectra of $[EuZn(L^9 - H)_3]^{2+}$ upon excitation through the ligand-centred $^1\pi\pi^*$ levels (λ_{exc} = 28 570–27 030 cm^{-1}). (*a*) Solid state, (*b*) 10^{-4} M in CH_3CN, (*c*) 10^{-4} M in H_2O and (*d*) 10^{-5} M in D_2O

depends almost exclusively on the pseudo-contact term since this proton is sufficiently remote from the paramagnetic Eu^{III} centre (eight bonds).[13] A similar behaviour is expected in $[EuZn(L^9 - H)_3]^{2+}$ and H^6 can be used as a structural probe. The comparison of the paramagnetic shifts of H^6 in $[EuZn(L^8)_3]^{5+}$ {1.89 ppm with respect to $[LaZn(L^8)_3]^{5+}$}[13] and in $[EuZn(L^9 - H)_3]^{2+}$ {3.78 ppm with respect to $[LaZn(L^9 - H)_3]^{2+}$, Table 1} indicates an increased pseudo-contact contribution in the latter complex strongly suggesting that H^6 is located closer to Eu^{III} [equation (1): δ_{ij}^{pc} depends on r_i^{-3}; C_j, *T* and *a* are expected to be similar in both complexes]. The large paramagnetic downfield shift of H^9 {9.83 ppm for $[EuZn(L^9 - H)_3]^{2+}$} compared to that observed in $[EuZn(L^8)_3]^{5+}$ (4.07 ppm)[13] has a related origin and leads to the conclusion that the replacement of the terminal carboxamide group in L^8 by a carboxylate in $[L^9 - H]^-$ results in a slight contraction of the structure along the C_3 axis in the resulting non-covalent podate $[LnZn(L^9 - H)_3]^{2+}$.

Photophysical properties of $[LnZn(L^9 - H)_3]^{2+}$ in solution

The absorption spectra of $[EuZn(L^9 - H)_3]^{2+}$ in solution (CH_3CN or H_2O) display intense $\pi \longrightarrow \pi^*$ transitions with two broad maxima centred at ≈41 000 cm^{-1} and 30 580 cm^{-1} (Table 2). The low-energy band corresponds to that found for $[EuZn(L^8)_3]^{5+}$ except for a slight red shift (1350 cm^{-1}) associated with the replacement of the carboxamide by a carboxylate group. Upon excitation through the ligand bands, we only observe strong red metal-centred luminescence pointing to an efficient ligand→Eu^{III} energy transfer process. The emission spectra of $[EuZn(L^9 - H)_3]^{2+}$ in CH_3CN and in H_2O are essentially identical and closely match the spectrum obtained for the solid-state sample suggesting that the same triple-helical

Table 3 Corrected integrated intensities (I_{rel}) and main identified Eu (^7F_j) energy levels (cm^{-1}, j = 1–4, origin $^7F_0$) for $[EuZn(L^9 - H)_3][ClO_4]_2 \cdot 7H_2O$ as calculated from luminescence spectra

	Solid state				Solution (10^{-4} M, 295 K)			
Level	10 K	I_{rel}	295 K	I_{rel}	CH_3CN	I_{rel}	H_2O	I_{rel}
λ_{exc}/cm^{-1}	17 224		17 235		28 409		27 398	
$^7F_0$*	17 224		17 235		17 237	0.003	17 231	0.01
$^7F_1$	284	1.00	277	1.00	287	1.00	283	1.00
	401		405		436		434	
	453		438					
$^7F_2$	976	0.78	970	1.32	988	1.43	1 003	0.78
	1 001		991				1 110	
	1 032		1 109		1 034			
	1 101				1 132			
	1 122							
$^7F_3$	1 833	0.07	1 834	0.08	1 847	0.08	1 834	0.06
$^7F_4$	2 705	1.03	2 718	1.39		1.22	2 718	1.05
	2 725		2 786		2 726		2 800	
	2 790		2 892		2 775		2 886	
	2 865sh		3 013				3 013	
	2 893				2 905			
	2 932sh				2 963			
	3 008				3 023			

* Energy of the $^5D_0 \longleftarrow {}^7F_0$ transition (given in cm^{-1}) taken as the reference.

structure is retained in both solvents and in the crystalline material (Fig. 3). Although a precise site symmetry determination is prohibited by the broad nature of the Eu emission bands in solution, their general features confirmed the trigonal geometry established by ^1H NMR spectroscopy. (*i*) The intensity of the $^5D_0 \longrightarrow {}^7F_0$ transition is weak but not negligible which is compatible with local C_3 or C_{3v} symmetries in which this transition is allowed (forbidden in D_3 or D_{3h} point groups).[15] (*ii*) The magnetic dipole transition $^5D_0 \longrightarrow {}^7F_1$ is split into two components A $\longrightarrow$ A and A $\longrightarrow$ E (labels for the C_3 point group) separated by $\Delta E = 151\ cm^{-1}$ (Table 3) which is characteristic for a trigonal arrangement as previously reported for $[EuZn(L^8)_3]^{5+}$ ($\Delta E = 140\ cm^{-1}$).[13] (*iii*) The electric dipole transition $^5D_0 \longrightarrow {}^7F_2$ displays two main components in water and a third band appearing as a shoulder on the low energy side of the most intense band in acetonitrile. This points to the existence of three allowed transitions assigned to the A $\longrightarrow$ A and the two A $\longrightarrow$ E components expected in C_3 symmetry.[13,15] Finally, a close scrutiny of the laser-excited excitation spectrum of the $^5D_0 \longleftarrow {}^7F_0$ transition reveals the existence of a unique component centred at 17 237 cm^{-1} [full width at half height (fwhh) = 22 cm^{-1}] in acetonitrile and 17 231 cm^{-1} (fwhh = 9 cm^{-1}) in water reflecting the presence of a single chemical environment around Eu^{III}, in agreement with the exclusive formation of the triple-helical non-covalent podate in these conditions.

According to Frey and Horrocks,[24] the energy of the $^5D_0 \longleftarrow {}^7F_0$ transition depends on the ability of each co-ordinating atom to produce a nephelauxetic effect $\tilde{\nu} - \tilde{\nu}_0 = C_{CN}\Sigma n_i\delta_i$ where C_{CN} is a constant depending upon the Eu^{III} co-ordination number (1.0 for CN = 9), n_i the number of atoms of type i, and $\tilde{\nu}_0 = 17\ 374\ cm^{-1}$ at 295 K[24] (the temperature dependence of $\tilde{\nu}$ is approximately 1 cm^{-1} per 24 K).[15] Taking into account the tabulated δ_i parameters for heterocyclic nitrogen atoms ($\delta_{HN} = -15.3$)[8–10,12,13] and for carboxylate oxygen atoms ($\delta_{CO_2} = -17.2$),[24] we calculate $\tilde{\nu} = 17\ 231\ cm^{-1}$ for nine-co-ordinate Eu^{III} in $[EuZn(L^9 - H)_3]^{2+}$ in perfect agreement with the observed value in water. The small discrepancy exhibited in acetonitrile (6 cm^{-1}) can be tentatively attributed to slight structural variations resulting from second-sphere interactions with the solvent since the δ_i parameters are very sensitive to the Eu–ligand bond distances.[9] This statement is confirmed by the weak, but significant variations observed in the relative integrated emission intensities of the $^5D_0 \longrightarrow {}^7F_j$ transitions of $[EuZn(L^9 - H)_3]^{2+}$ in the two solvents (Table 3). The long lifetimes of the Eu ($^5D_0$) level in solution ($\tau_{D_2O} = 4.48$ ms, $\tau_{CH_3CN} = 3.60$ ms and $\tau_{H_2O} = 2.43$ ms) indicate that inner-sphere solvent interaction is prevented by the tight wrapping of the three ligand strands. Using the empirical equation of Horrocks and Sudnick,[25] $q = A_{Eu}(\tau^{-1}_{H_2O} - \tau^{-1}_{D_2O})$ with $A_{Eu} = 1.05$ leads to $q = 0.2$ water molecule, which strongly suggests that only second-sphere quenching mechanisms are operative[14] in agreement with the expected nine-co-ordinate tricapped trigonal prismatic Eu^{III} site [three N (benzimidazole) and three O (carboxylate) occupying the vertices of the prism and three N (pyridine) capping the faces]. Successive dilutions of the sample in H_2O or in D_2O (10^{-4}–10^{-8} M) do not alter the emission spectra except for the expected decrease in intensity which demonstrates the unprecedented stability of the non-covalent podate $[EuZn(L^9 - H)_3]^{2+}$ in solution. For comparison purposes, the best result with this class of supramolecular complexes was previously obtained for $[EuZn(L^8)_3]^{5+}$ which displayed significant decomplexation at 10^{-5} M in weakly co-ordinating anhydrous acetonitrile.[13]

The quantum yield of a 10^{-4} M solution of $[EuZn(L^9 - H)_3]^{2+}$ in acetonitrile relative to $[Eu(terpy)_3]^{3+}$ (10^{-3} M) amounts to $\Phi_{rel} = 1.00$ which corresponds to a three-fold increase compared to $[EuZn(L^8)_3]^{5+}$ (Table 4).[13] In fact, the total relative emission intensity obtained by multiplying the quantum yield by the efficiency of light absorption (*i.e.* the ratio of the molar absorption coefficients of the sample and the reference) amounts to 6.7 for $[EuZn(L^8)_3]^{5+}$ [13] and 14.0 for $[EuZn(L^9 - H)_3]^{2+}$. Upon addition of water into the acetonitrile solution, the quantum yield slightly decreases as does the Eu ($^5D_0$) lifetime (Table 4, Fig. 4) in agreement with second-sphere effects. In pure water, the quantum yield falls to $\Phi_{ref} = 0.47$ but the solution remains strongly luminescent, in contrast to aqueous $[Eu(terpy)_3]^{3+}$ which is fully decomplexed and non-luminescent in these conditions.

Photophysical properties of $[LnZn(L^9 - H)_3][ClO_4]_2$ in the solid state

The reflectance spectra of the free ligand is characterized by a broad $\pi \longrightarrow \pi^*$ transition centred at 31 250 cm^{-1} which is shifted toward low energy upon co-ordination to Ln^{III} (Ln = La or Eu) and Zn^{II} in $[LnZn(L^9 - H)_3][ClO_4]_2$ (Table 2) in contrast to the slight blue shift found for $[LnZn(L^8)_3][ClO_4]_5$.[13] A weak luminescence is observed for L^9 at 77 K upon excitation of its singlet state leading to a broad emission band centred around

Table 4 Quantum yields (Φ_{rel}) relative to $[Eu(terpy)_3]^{3+}$ (terpy = 2,2′ : 6′,2″ terpyridine) and lifetimes (τ) of the Eu ($^5D_0$) level for $[EuZn(L^9 - H)_3]^{2+}$ at 298 K[a]

Compound	Solvent	Concentration/M	Added H_2O/M	λ_{exc}/nm	ε_{exc}/M^{-1} cm^{-1}	Φ[b]	τ/ms
$[Eu(terpy)_3]^{3+}$[c]	CH_3CN	10^{-3}	0	371	549	1.00	2.51(1)
$[EuZn(L^9 - H)_3]^{2+}$	CH_3CN	10^{-4}	0	362	7680	1.00	3.60(2)
$[EuZn(L^9 - H)_3]^{2+}$	CH_3CN	10^{-4}	1	362	7640	1.03	3.27(2)
$[EuZn(L^9 - H)_3]^{2+}$	CH_3CN	10^{-4}	2	362	7780	0.87	3.14(2)
$[EuZn(L^9 - H)_3]^{2+}$	CH_3CN	10^{-4}	10	362	7600	0.80	2.76(2)
$[EuZn(L^9 - H)_3]^{2+}$	CH_3CN	10^{-4}	28	362	7780	0.70	2.70(2)
$[EuZn(L^9 - H)_3]^{2+}$	H_2O	10^{-4}	—	367	8510	0.47	2.43(2)
$[EuZn(L^9 - H)_3]^{2+}$	D_2O	10^{-4}	—	308	—	—	4.48(1)
$[EuZn(L^8)_3]^{5+}$[d]	CH_3CN	10^{-4}	0	380	2750	0.29	2.90(2)
$[EuZn(L^8)_3]^{5+}$[d]	CH_3CN	10^{-4}	0.93	380	2750	0.29	—

[a] The quantum yields of $[Eu(terpy)_3]^{3+}$ relative to an aerated water solution of $[Ru(bipy)_3]^{2+}$ (bipy = 2,2′-bipyridine) is 0.47 which allows the calculation of absolute quantum yields.[26] [b] Relative errors on Φ_{rel} are typically 10–15%. [c] Quantum yields are determined relative to $[Eu(terpy)_3]^{3+}$ 10^{-3} M solution to avoid decomplexation. [d] Taken from ref. 13.

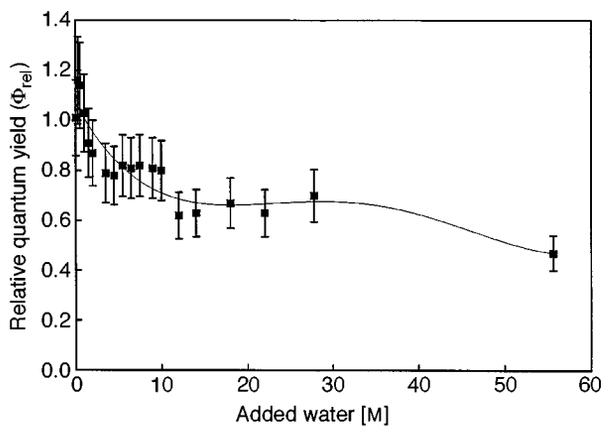

Fig. 4 Quantum yield relative to $[Eu(terpy)_3]^{3+}$ for 10^{-4} M solution of $[EuZn(L^9 - H)_3]^{2+}$ in acetonitrile measured *versus* the concentration of added water

24 750 cm^{-1} and assigned as arising from the $^1\pi\pi^*$ excited state. Pulsed (10 Hz) laser irradiation at 32 468 cm^{-1} combined with time-resolved detection of the signal evidences a weak, but structured and long-lived emission band at 21 980 cm^{-1} (0-phonon; vibronic progression ≈1350 cm^{-1}) assigned to the triplet state. The observed biexponential luminescence decay at 10 K [τ_1 = 14(2) ms and τ_2 = 1050(30) ms] is typical of these bidentate–tridentate receptors [τ_1 = 41(2) ms and τ_2 = 560(18) ms for L^8, Table 2][13] and has been tentatively attributed as arising from the two different segments of the ligand.[13] In $[LaZn(L^9 - H)_3][ClO_4]_2$, the $^1\pi\pi^*$ and $^3\pi\pi^*$ emission bands at 77 K are not significantly altered except for a slight red shift of *ca.* 500–700 cm^{-1}. However, the complexation perturbs the electron density thus inducing an efficient non-radiative deactivation of the $^3\pi\pi^*$ state (Table 2). In $[EuZn(L^9 - H)_3][ClO_4]_2$, the emission of the triplet state vanishes and a faint residual emission of the singlet state is observed at 22 940 cm^{-1}. The emission spectrum is dominated by the Eu^{III}-centred $^5D_0 \longrightarrow {}^7F_j$ (j = 0–6) transitions pointing again to an efficient antenna effect in the complex (Fig. 5).

Although weak, the $^5D_0 \longleftrightarrow {}^7F_0$ transition is detected as a single symmetrical band both in the emission and excitation spectra (10 K, 17 224 cm^{-1}, fwhh = 17.0 cm^{-1}; 295 K, 17 235 cm^{-1}, fwhh = 16.3 cm^{-1}) compatible with a unique Eu^{III} site in the powdered sample. However, the large fwhh suggests a statistical distribution of molecules having somewhat different conformation: a characteristic of either amorphous materials and/or complexes with a large fluxionality.[27] The energy of the 0–0 transition is close to that found in solution and fits the values calculated with the Frey and Horrocks equation[24] pointing to identical Eu^{III} co-ordination spheres in both solid and solution state. The lifetime of the Eu ($^5D_0$) state measured upon excitation of the $^5D_0 \longleftarrow {}^7F_0$ transition does not depend on temperature (10–295 K) and amounts to 2.40 ms, a value close to that measured for $[EuZn(L^9 - H)_3]^{2+}$ in water (Table 5) which indicates that (*i*) the vibrational modes of the complex do not participate efficiently to the radiationless decay and (*ii*) the seven water molecules of the solid-state sample are interstitial and produce only second-sphere interactions. Excitation through the $^1\pi\pi^*$ ligand state produces significantly longer lifetimes suggesting that the triplet state is involved in the ligand $\longrightarrow$ Eu energy transfer process.[15,28] Finally, the emission spectrum of $[EuZn(L^9 - H)_3][ClO_4]_2$ displays the characteristics associated with pseudo-trigonal symmetry as previously discussed for $[EuZn(L^9 - H)_3]^{2+}$ in solution and for $[EuZn(L^8)_3][ClO_4]_5$ in the solid state.[13] The magnetic dipole transition $^5D_0 \longrightarrow {}^7F_1$ is comprised of two main bands attributed to A $\longrightarrow$ A and A $\longrightarrow$ E components in C_3 point group.[15] The A level is located at 284 cm^{-1} (10 K) above the $^7F_0$ (A) level and is separated by 117 cm^{-1} from the E level which is further split into two closely spaced

Table 5 Lifetimes τ (ms) of the Eu ($^5D_0$) excited level for $[EuZn(L^9 - H)_3][ClO_4]_2 \cdot 7H_2O$ in the solid state under various excitation conditions (analysing wavelength set at the maximum of the $^5D_0 \longrightarrow {}^7F_2$ transition)

T/K	λ_{exc}/cm^{-1}	τ/ms
10	17 238	2.41(18)
10	32 468	2.99(9)
77	17 238	2.41(38)
77	32 468	2.95(7)
295	17 248	2.42(10)
295	26 810	2.39(14)
295	32 468	2.60(17)

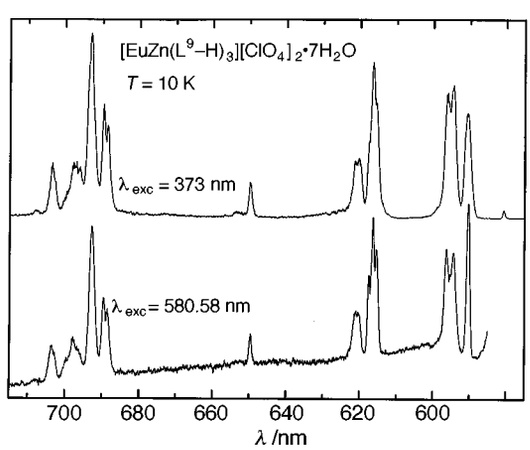

Fig. 5 Emission spectra of $[EuZn(L^9 - H)_3][ClO_4]_2 \cdot 7H_2O$ at 10 K under (*a*) irradiation of the ligand-centred excited states (λ_{exc} = 26 810 cm^{-1}) and (*b*) direct laser excitation of the $^7F_0 \longrightarrow {}^5D_0$ transition (λ_{exc} = 17 224 cm^{-1})

components ($\Delta E = 52$ cm^{-1}) as a result of small distortions from the idealized trigonal symmetry. A similar splitting pattern has been observed in $[EuZn(L^8)_3][ClO_4]_5$ (117 and 21 cm^{-1})[13] where Eu^{III} is located in a site close to C_3 symmetry. The increased splitting of the E components in $[EuZn(L^9 - H)_3][ClO_4]_2$ might indicate a larger deviation from the expected trigonal symmetry in the latter complex. The analysis of the $^5D_0 \longrightarrow {}^7F_2$ transition is complicated by vibronic transitions, but we observe five strong bands (10 K) from which two doublets are attributed to the allowed electric dipole A $\longrightarrow$ E transitions (first doublet: sublevels 976 and 1001 cm^{-1}, splitting = 25 cm^{-1} and second doublet: sublevels 1101 and 1122 cm^{-1}, splitting = 21 cm^{-1}; Table 3) and the singlet is associated with the A $\longrightarrow$ A transition (sublevel: 1032 cm^{-1}). A closely related splitting pattern has been observed for the pseudo-C_3 symmetrical complex $[EuZn(L^8)_3][ClO_4]_5$ with separations of respectively 18 and 22 cm^{-1} between the components of the doublets.[13] Higher symmetries D_3 and D_{3h} are precluded since only two and one component are expected for the $^5D_0 \longrightarrow {}^7F_2$ transition as found in $[Eu(L^2)_3]^{3+}$.[8] The $^5D_0 \longrightarrow {}^7F_4$ transition displays at least seven components in qualitative good agreement with the postulated trigonal symmetry (six transitions expected for C_3).

Conclusion

The replacement of the neutral carboxamide group in L^8 by a negatively charged carboxylate in $[L^9 - H]^-$ has beneficial effects on both the stability and the emission properties of the non-covalent lanthanide podate $[EuZn(L^9 - H)_3]^{2+}$. The latter complex possesses a ligand-centred 0-phonon triplet state located 4050 cm^{-1} above the Eu ($^5D_0$) state which is suitable to ensure efficient, fast and irreversible ligand $\longrightarrow$ Eu^{III} energy transfer according to the criteria proposed by Reinhoudt and co-workers [$\Delta E = E$ ($^3\pi\pi^*$) $- E$ ($^5D_0$) > 3500 cm^{-1}].[29] Compared to $[EuZn(L^8)_3]^{5+}$ ($\Delta E = 2730$ cm^{-1}),[13] the energy gap in $[EuZn(L^9 - H)_3]^{2+}$ is significantly increased which limits energy back transfer and induces a good match between the energy of the donor ($^3\pi\pi^*$) and the acceptor [Eu ($^5D_{0,1}$)] levels. As a consequence, $[EuZn(L^9 - H)_3]^{2+}$ is three times more luminescent than $[EuZn(L^8)_3]^{5+}$ in acetonitrile, but the most fascinating effect concerns its stability in solution. While $[EuZn(L^8)_3]^{5+}$ is significantly decomplexed in weakly co-ordinating acetonitrile at a concentration of 10^{-5} M and fully decomplexed in water, the carboxylate groups in $[EuZn(L^9 - H)_3]^{2+}$ improve the stability and the resistance toward hydrolysis, the latter complex remaining intact in water and still displaying a strong red emission characteristic of the C_3-symmetrical lanthanide podate for concentrations as low as 10^{-7}–10^{-8} M. The quantum yield of $[EuZn(L^9 - H)_3]^{2+}$ is slightly reduced in water (compared to acetonitrile) as a result of second-sphere effects, but the three wrapped ligand strands efficiently protect Eu^{III} from external interactions. The introduction of carboxylate groups in segmental ligands represents a crucial step in the development of stable self-assembled non-covalent lanthanide podates with tunable and luminescent Ln^{III} sites suitable (*i*) for the investigation of intra- and inter-molecular d $\longleftrightarrow$ f energy transfer[20] and (*ii*) for the synthesis of luminescent probes and sensors in aqueous media.[13] This approach is currently limited by the poor solubility of heterocyclic carboxylate-containing receptors, but new strategies aiming at the development of highly water-soluble functional lanthanide podates are under investigation in our laboratories.

Experimental

Solvents and starting materials

These were purchased from Fluka AG (Buchs, Switzerland) and used without further purification unless otherwise stated. Acetonitrile, nitromethane, dimethyl sulfoxide and triethylamine were distilled from CaH_2 and the ligand 2-[6-(diethylcarbamoyl)pyridin-2-yl]-1,1′-dimethyl-2′-(5-methylpyridin-2-yl)-5,5′-methylenebis(1*H*-benzimidazole) (L^8) was prepared according to a literature procedure.[13] The perchlorate salts $Ln(ClO_4)_3 \cdot 7H_2O$ (Ln = La or Eu) were prepared from the corresponding oxides[30] (Glucydur, 99.99%).

Preparation

2-(6-Carboxypyridin-2-yl)-1,1′-dimethyl-2′-(5-methylpyridin-2-yl)-5,5′-methylenebis(1*H*-benzimidazole) (L^9). A solution of L^8 (100 mg, 184 μmol) in ethanol–water (25:100 cm^3) containing potassium hydroxide (85%, 6.58 g, 100 mmol) was refluxed for 14 h. Ethanol was distilled and the aqueous phase neutralized (pH = 3) with concentrated hydrochloric acid. The resulting precipitate was filtered off, washed with water and ethanol and crystallized from hot dimethyl sulfoxide–water to give 87 mg (168 μmol, yield 91%) of L^9 as a white powder, m.p. >210 °C. ^{1}H NMR in $(CD_3)_2SO$: δ 2.39 (3 H, s), 4.18 (3 H, s), 4.22 (2 H, s), 4.32 (3 H, s), 7.23 (1 H, dd, $J^3 = 8$, $J^4 = 1.2$), 7.27 (1 H, dd, $J^3 = 8$, $J^4 = 1.2$), 7.51 (1 H, d, $J^3 = 8$), 7.53 (1 H, d, $J^3 = 8$), 7.57 (1 H, s), 7.62 (1 H, s), 7.79 (1 H, dd, $J^3 = 8$, $J^4 = 1.2$), 8.12 (1 H, dd, $J^3 = 8$, $J^4 = 1.2$), 8.16 (1 H, t, $J^3 = 8$), 8.18 (1 H, d, $J^3 = 8$), 8.48 (1 H, dd, $J^3 = 8$, $J^4 = 1.2$ Hz), 8.56 (1 H, s br). Electron impact mass spectrum: *m*/*z* 488 (M^+).

$[LnZn(L^9 - H)_3][ClO_4]_2 \cdot nH_2O$ ($n = 6.6$, Ln = La; $n = 7$, Ln = Eu). A solution of $Ln(ClO_4)_3 \cdot nH_2O$ (20.5 μmol) (Ln = La or Eu) in nitromethane (100 μl) and $Zn(ClO_4)_2 \cdot 6H_2O$ (7.63 mg, 20.5 μmol) in acetonitrile (50 μl) was added to a suspension of L^9 (30 mg, 61.4 μmol) in nitromethane (4 cm^3). Triethylamine (6.2 mg, 61.4 μmol) in nitromethane (120 μl) was added in three portions and the resulting solution stirred until it became clear. Filtration, evaporation to dryness followed by redissolution in nitromethane (4 cm^3) and slow diffusion of diethyl ether for 1 d gave 15.4 mg (7.76 μmol, yield 38%, Ln = La) and 17.5 mg (8.73 μmol, yield 43%, Ln = Eu) of $[LnZn(L^9 - H)_3][ClO_4]_2 \cdot nH_2O$ ($n = 6.6$, Ln = La; $n = 7$, Ln = Eu) as white microcrystalline powders (Found: C, 52.92; H, 4.53; N, 12.64. Calc. for $C_{87}H_{69}Cl_2LaN_{18}O_{14}Zn \cdot 6.6H_2O$: C, 52.65; H, 4.17; N, 12.70%. ES mass spectrum (10^{-4} M, CH_3CN): *m*/*z* 833.4 {$[LaZn(L^9 - H)_3]^{2+}$, 100%}. Found: C, 52.20; H, 3.94; N, 12.56. Calc. for $C_{87}H_{69}Cl_2EuN_{18}O_{14}Zn \cdot 7H_2O$: C, 52.12; H, 4.17; N, 12.57%. ES mass spectrum (10^{-4} M, CH_3CN): *m*/*z* 840.0 {$[EuZn(L^9 - H)_3]^{2+}$, 100%}).

CAUTION. Perchlorate salts combined with organic ligands are potentially explosive and should be handled with the necessary precautions.[31]

Spectroscopic and analytical measurements

Reflectance spectra were recorded as finely grounded powders dispersed in MgO (5%) with MgO as reference on a Perkin-Elmer Lambda 19 spectrophotometer equipped with a Labsphere RSA-PE-19 integration sphere. Electronic spectra in the UV/VIS range were recorded at 20 °C from 10^{-3} M acetonitrile solutions with Perkin-Elmer Lambda 5 and Lambda 7 spectrometers using quartz cells of 0.1 and 0.01 cm path length. Infrared spectra were obtained from KBr pellets with a Perkin-Elmer 883 spectrometer. Proton NMR spectra were recorded at 25 °C on a Broadband Varian Gemini 300 spectrometer. Chemical shifts are given in ppm with respect to internal $SiMe_4$. Electron impact mass spectra (70 eV ≈ 1.12 × 10^{-17} J) were recorded with VG-7000E and Finnigan-4000 instruments. Pneumatically-assisted electrospray (ES) mass spectra were recorded from acetonitrile solutions on a API III and API 300 tandem mass spectrometer (PE Sciex) by infusion at 4–10 μl min^{-1}. The spectra were recorded under low up-front declustering as previously described.[13,19] The experimental procedures for high-resolution, laser-excited luminescence

measurements have been published previously.[32] Solid-state samples were finely powdered and low-temperature (77 or 10 K) was achieved by means of a Cryodyne Model 22 closed-cycle refrigerator from CTI Cryogenics. Luminescence spectra were corrected for the instrumental function, but not excitation spectra. Lifetimes are averages of at least 3–5 independent determinations. Ligand excitation and emission spectra were recorded on a Perkin-Elmer LS-50 spectrometer equipped for low-temperature measurements. The relative quantum yields were calculated using the following formula:[10] $Q_x/Q_r = \langle A_r(\lambda_r)/A_x(\lambda_x)\rangle\langle I(\lambda_r)/I(\lambda_x)\rangle\langle n^2_x/n^2_r\rangle\langle D_x/D_r\rangle$ where subscript r stands for the reference and x for the samples; A is the absorbance at the excitation wavelength, I is the intensity of the excitation light at the same wavelength, n is the refractive index (1.341 in acetonitrile and 1.333 in water) and D is the measured integrated luminescence intensity. Elemental analyses were performed by Dr. H. Eder from the Microchemical Laboratory of the University of Geneva.

Acknowledgements

We are grateful to Ms. Véronique Foiret for her technical assistance. C. P. thanks the Werner Foundation for a fellowship, and J.-C. B. thanks the Fondation Herbette (Lausanne) for the gift of spectroscopic equipment. This work is supported through grants from the Swiss National Science Foundation.

References

1 C. Piguet, *Chimia*, 1997, **51**, 240; J.-C. G. Bünzli, S. Petoud, C. Piguet and F. Renaud, *J. Alloys Compd.*, 1997, **249**, 14; C. Piguet and J.-C. G. Bünzli, *Eur. J. Solid State Inorg. Chem.*, 1996, **33**, 165; C. Piguet, *Chimia*, 1996, **50**, 144.
2 V.-M. Mukkala, M. Helenius, I. Hemmilä, J. Kankare and H. Takalo, *Helv. Chim. Acta*, 1993, **76**, 1361; H. Takalo, V.-M. Mukkala, L. Meriö, J. C. Rodriguez-Ubis, R. Sedano, O. Juanes and E. Brunet, *Helv. Chim. Acta*, 1997, **80**, 372.
3 J. Coates, P. G. Sammes and R. M. West, *J. Chem. Soc.*, *Perkin Trans. 2*, 1996, 1275; 1996, 1283.
4 J. C. Rodriguez-Ubis, R. Sedano, G. Barroso, O. Juanes and E. Brunet, *Helv. Chim. Acta*, 1997, **80**, 86.
5 J. B. Lamture, Z. Zhou, S. Kumar and T. G. Wenzel, *Inorg. Chem.*, 1995, **34**, 864; P. A. Brayshaw, J.-C. G. Bünzli, P. Froidevaux, J. M. Harrowfield, Y. Kim and A. N. Sobolev, *Inorg. Chem.*, 1995, **34**, 2068; J. M. Harrowfield, Y. Kim, B. W. Skelton and A. H. White, *Aust. J. Chem.*, 1995, **48**, 807 and refs. therein; I. Grenthe, *J. Am. Chem. Soc.*, 1961, **83**, 360; C. N. Reilley, B. W. Good and J. F. Desreux, *Anal. Chem.*, 1975, **47**, 2110; D. H. Metcalf, J. P. Bolender, M. S. Driver and F. S. Richardson, *J. Phys. Chem.*, 1993, **97**, 553.
6 D. A. Durham, G. H. Frost and F. A. Hart, *J. Inorg. Nucl. Chem.*, 1969, **31**, 833; G. H. Frost, F. A. Hart and M. B. Hursthouse, *Chem. Commun.*, 1969, 1421; R. D. Chapman, R. T. Loda, J. P. Riehl and R. W. Schwartz, *Inorg. Chem.*, 1984, **23**, 1652.
7 C. Mallet, R. P. Thummel and C. Hery, *Inorg. Chim. Acta*, 1993, **210**, 223.
8 F. Renaud, C. Piguet, G. Bernardinelli, J.-C. G. Bünzli and G. Hopfgartner, *Chem. Eur. J.*, 1997, **3**, 1646.
9 F. Renaud, C. Piguet, G. Bernardinelli, J.-C. G. Bünzli and G. Hopfgartner, *Chem. Eur. J.*, 1997, **3**, 1660.
10 C. Piguet, A. F. Williams, G. Bernardinelli and J.-C. G. Bünzli, *Inorg. Chem.*, 1993, **32**, 4139; C. Piguet, J.-C. G. Bünzli, G. Bernardinelli, C. G. Bochet and P. Froidevaux, *J. Chem. Soc.*, *Dalton Trans.*, 1995, 83.
11 C. Piguet, G. Bernardinelli and G. Hopfgartner, *Chem. Rev.*, 1997, **97**, 2005; E. C. Constable, *Prog. Inorg. Chem.*, 1994, **42**, 67; E. C. Constable, in *Comprehensive Supramolecular Chemistry*, eds. J. L. Atwood, J. E. D. Davies, D. D. MacNicol and F. Vögtle, Pergamon, Oxford, 1996, ch. 6.
12 C. Piguet, G. Hopfgartner, A. F. Williams and J.-C. G. Bünzli, *J. Chem. Soc.*, *Chem. Commun.*, 1995, 491; C. Piguet, E. Rivara-Minten, G. Hopfgartner and J.-C. G. Bünzli, *Helv. Chim. Acta*, 1995, **78**, 1541.
13 C. Piguet, G. Bernardinelli, J.-C. G. Bünzli, S. Petoud and G. Hopfgartner, *J. Chem. Soc.*, *Chem. Commun.*, 1995, 2575; C. Piguet, J.-C. G. Bünzli, G. Bernardinelli, G. Hopfgartner, S. Petoud and O. Schaad, *J. Am. Chem. Soc.*, 1996, **118**, 66.
14 D. Parker and J. A. Gareth-Williams, *J. Chem. Soc.*, *Dalton Trans.*, 1996, 3613; S. L. Wu and W. de W. Horrocks, jun., *J. Chem. Soc.*, *Dalton Trans.*, 1997, 1497; D. M. Rudkevich, N. Verboom, E. van der Tol, C. J. van Staveren, F. M. Kasperstein, J. W. Verhoeven and D. N. Reinhoudt, *J. Chem. Soc.*, *Perkin Trans. 2*, 1995, 131.
15 J.-C. G. Bünzli, in *Lanthanide Probes in Life*, *Chemical and Earth Sciences*, eds. J.-C. G. Bünzli and G. R. Choppin, Elsevier, Amsterdam, 1989, ch. 7.
16 C. Piguet, B. Bocquet and G. Hopfgartner, *Helv. Chim. Acta*, 1994, **77**, 931; P. G. Gassman, P. K. G. Hodgson and R. J. Balchanis, *J. Am. Chem. Soc.*, 1976, **98**, 1276.
17 M. M. Harding, U. Koert, J.-M. Lehn, C. Piguet, A. Rigault and J. Siegel, *Helv. Chim. Acta*, 1991, **74**, 594.
18 K. Nakamoto, *Infrared and Raman Spectra of Inorganic and Coordination Compounds*, J. Wiley, New York, Chichester, Brisbane and Toronto, 3rd edn., 1972, p. 142.
19 G. Hopfgartner, C. Piguet and J. D. Henion, *J. Am. Soc. Mass Spectrom.*, 1994, **5**, 748.
20 C. Piguet, J.-C. G. Bünzli, G. Bernardinelli, G. Hopfgartner and E. Rivara-Minten, *J. Chem. Soc.*, *Dalton Trans.*, 1997, 421.
21 C. Piguet, G. Hopfgartner, B. Bocquet, O. Schaad and A. F. Williams, *J. Am. Chem. Soc.*, 1994, **116**, 9092.
22 I. Bertini and C. Luchinat, *NMR of Paramagnetic Molecules in Biological Systems*, Benjamin/Cummings Publishing Co., Menlo Park, CS, 1986, ch. 10; I. Bertini, P. Turano and A. J. Vila, *Chem. Rev.*, 1993, **93**, 2833.
23 B. J. Bleaney, *J. Magn. Reson.*, 1972, **8**, 91; J. Reuben and G. A. Rigavish, *J. Magn. Reson.*, 1980, **39**, 421.
24 S. T. Frey and W. de W. Horrocks, jun., *Inorg. Chim. Acta*, 1995, **229**, 383.
25 W. de W. Horrocks, jun. and D. R. Sudnick, *J. Am. Chem. Soc.*, 1979, **101**, 334; W. de W. Horrocks, jun. and D. R. Sudnick, *Science*, 1979, **206**, 1194; W. de W. Horrocks, jun. and D. R. Sudnick, *Acc. Chem. Res.*, 1981, **14**, 384.
26 K. Nakamura, *Bull. Chem. Soc. Jpn.*, 1982, **55**, 2697.
27 J.-C. G. Bünzli and G. O. Pradervand, *J. Chem. Phys.*, 1986, **85**, 2489; J.-C. G. Bünzli, D. Plancherel and G. O. Pradervand, *J. Phys. Chem.*, 1989, **93**, 980; F. Nicolo, D. Plancherel, G. Chapuis and J.-C. G. Bünzli, *Inorg. Chem.*, 1988, **27**, 3518.
28 N. Sabbatini, M. Guardigli and J.-M. Lehn, *Coord. Chem. Rev.*, 1993, **123**, 201.
29 F. J. Steemers, W. Verboom, D. N. Reinhoudt, E. B. Vandertol and J. W. Verhoeven, *J. Am. Chem. Soc.*, 1995, **117**, 9408.
30 J. F. Desreux, in *Lanthanide Probes in Life*, *Chemical and Earth Sciences*, eds. J.-C. G. Bünzli and G. R. Choppin, Elsevier, Amsterdam, 1989, ch. 2, p. 43.
31 W. C. Wolsey, *J. Chem. Educ.*, 1973, **55**, A355.
32 C. Piguet, A. F. Williams, G. Bernardinelli, E. Moret and J.-C. G. Bünzli, *Helv. Chim. Acta*, 1992, **75**, 1697.

Received 27*th August* 1997; *Paper* 7/06256G